RSC Advances

ROYAL SOCIETY OF CHEMISTRY

www.rsc.org/advances

Preparation and Evaluation of a Novel pADM-derived Micro-and nano Electrospun Collagen Membrane

Xinhua Liu [a,b], Weihua Dan [a,b], Haiyan Ju [a,b], Nianhua Dan [a,b*], Juxia Gong[a,b]

[a] Key Laboratory for Leather Chemistry and Engineering of the Education Ministry, Sichuan University, Chengdu, Sichuan 610065, China

[b] Research Center of Biomedical Engineering, Sichuan University, Chengdu, Sichuan 610065, China

Corresponding author at: Department of Biomass Chemistry and Engineering,Sichuan University, Chengdu, Sichuan 610065, China; Tel.: +86 28 85408988; fax: +86 28 85408988.

E-mail addresses: danweihua scu@126.com (W. Dan), liuxinhuam@163.com (N. Dan).

Abstract

As the three-dimensional (3D) architecture of porcine acellular dermal matrix (pADM) mimics the biological characteristics of the native extracellular matrix (ECM), then it has been extensively utilized as a tissue scaffold. In this study, a novel pADM-derived micro-and nano electrospun collagen membrane (PDEC) was sucessfully prepared by the electrospinning technique using porcine acellular dermal matrix (pADM) as raw material and 1,1,1,3,3,3-hexafluoro-2-propanol (HIFP) as solvent，which was by scanning electron microscopy (SEM) analysis. Meanwhile, in contrast, another collagen-derived electrospun collagen (CDEC) was also

fabricated by using pure porcine collagen as raw material. The structure and composition of the PDEC and CDEC were measured by fourier transform infrared (FTIR) spectroscopy, SDS–PAGE gel electrophoresis, specific intrinsic viscosity and atomic force microscope (AFM). Results indicate that the structure integrity of the PDEC is almost maintained and just only a small amount of the PDEC is destroyed into gelatin, while almost all the CDEC is degraded. Moreover, the result of circular dichroism (CD) analysis also demonstrates that the PDEC possesses a higher content of α-helix structure but a less β-turn structure. Additionally, the results of the ultrasensitive differential scanning calorimetry (US-DSC) and XRD analysis also suggest that the thermal stability and crystallization of the PDEC have little differences from collagen. Moreover, the mechanical properties of PDEC are significantly enhanced compared to that of CDEC. Above all, the results obtained in the MTT study also indicate that the cytotoxicity of the PDEC has almost the same good biological activity as natural porcine collagen, which is superior than that of CDEC obviously. In conclusion, our study provides a new pADM-derived electrospun collagen of which its triple helical structure has seldom been damaged and thus it can be applied as a novel electrospun collagen scaffold for tissue engineering materials.

KEYWORDS*:* Porcine Acellular Dermal Matrix (pADM)*;* Structure*;* Electrospinning

1. Introduction

Recently, more and more ultrathin fiber networks derived from diverse materials [1-4] are fabricated by the electrospinning technique. As the electrospun

scaffold has a unique microstructure and appropriate mechanical properties, such nanofiber biomaterials may represent a kind of potential tissue engineering scaffolds [5-6] and promising functional biomaterials such as wound dressings [7] and carrier for drug delivery [8]. It is worthy to note that electrospun collagen has received a great deal of attentions currently on account of its superior biological properties [9]. Nonetheless, whatever the reported solvent (e.g. acidic water, 1,1,1,3,3,3-hexafluoro-2-propanol, trifluoroethanol or ethanol–phosphate buffer) is utilized in the process of electrostatic spinning, the resulting electrospun collagen inevitably exhibits poor mechanical firmness and insufficient resistance in water to withstand dissolution [10-13]. Moreover when HFIP or TFE is used as a solvent, earlier study [14] showes that 99% of collagen is apparently lost during the electro-spinning process. Electrospun collagen out of fluoroalcohols results in the creation of gelatin, which is derived from denatured collagen and characterized by destroyed α-chains, disrupted triple-helical, damaged fibrillar structure and lacking internal structure or configurational order [15]. Furthermore, electrospun collagen using either HIFP or TFE as solvent has been reported to yield collagenous nano-fibers, which do not swell in aqueous media like other collagenous structures [16-18], but instead are soluble in water, tissue fluids or blood [19-21]. This may hinder the development of electrospun collagen tremendously. More importantly, applications of electrospun collagen are also limited in biomedical field due to its poor biodegradable properties [15]. Therefore these issues need to be resolved urgently.

Porcine acellular dermal matrix (pADM) has been extensively utilized as tissue

scaffold on account of its specific three-dimensional (3D) architecture that mimics the biological characteristics of the native extracellular matrix (ECM) similarly [22-24]. pADM is prepared from the pigskin by using physical, chemical, biological and other methods to eliminate a whole layer of the epidermis and all cellular components of the dermis, and thus retain the collagen fibers and the basic organization structure finally [25]. Therefore the immune activity of pADM could almost be negligible, likewise, either the specific allogeneic cellular immune response or non-specific foreign body reaction against tissue transplantation would be induced [26]. The main component of pADM is collagen fibers and further the collagen fibers are the aggregated structure of collagen molecules. According to our previous report [28], the pADM also inherits the fantanstic biocompatiblity of collagen. Furthermore, compared to natural collagen molecules, the structure of pADM remains more stable in different chemical environments apparently due to its multi-level aggregation structure. Considering the performance standpoint, superior mechanical properties, biodegradability, better crystallinity and thermal stability are exhibited in the porcine acellular dermal matrix, which make it more suitable for the preparation of electrospun collagen [27].

Aming at solving the problems mentioned above, porcine acellular dermal matrix, which has a more stable structure than collagen molecule and is not easy for HFIP to destroy its aggregation structure, is chosen as a model collagen used in this study. Two types of electrospun collagen derived from pADM and pure collagen were prepared and their structural integrity and configuration were evaluated with fourier

transform infrared spectroscopy (FTIR), Circular dichroism (CD), Sodium dodecyl sulfate-polyacrylamide gel electrophoresis (SDS-PAGE), US-DSC, X-ray diffraction (XRD), SEM and atomic force microscopy (AFM). Moreover, the mechanical characteristics of the pADM-derived electrospun collagen membrane and collagen-derived electrospun collagen membrane were appraised with an electronic universal material tensile machine. Further, the cytotoxicity of the two electrospun collagen was also evaluated by MTT assay. Accordingly, this work is focused on preparing a novel pADM-derived micro-nano electrospun collagen membrane which may maintain the ingeterity of collagen's structure and desirable fibrous morphology. Therefore, it may be of benefit for the fabrication of novel biological nano-scaffold materials.

2. Experiments

2.1 Materials

Porcine acellular dermal matrix (pADM) scaffolds and pure collagen used in this work were self-prepared according to our previous report [28-29] or invention patent (CN1569260). As shown in Figure 1, the results of histological observation, chemical analysis and electron microscopy observation confirm that miscellaneous structural proteins, various cells, fat and other non-collagenous materials are effectively depleted and the contents of fat, ash, protein and moisture in pADM are 0.71%, 2.04%, 80.12% and 20.63%, respectively. 1,1,1,3,3,3-hexafluoro-2-propanol was obtained from HWRK Chem Co., LTD (Beijing, China). Unless noted otherwise, all

chemicals and reagents were purchased from Sigma–Aldrich (St. Louis, MO, USA) .

2.2 Electrospinning

A certain mass of pADM pieces (2.0 mm×2.0 mm) and pure porcine collagen were both dissolved in HIFP at a concentration of 4% (g/ml). Before electrospinning, the solutions were sufficiently stirred at 4℃ for 24 h. Then the electrospinning experiment was conducted at room temperature. The solutions were filled into two 5.0 mL plastic syringes with a blunt-end needle having an inner diameter of 0.46 mm. Meanwhile a syringe pump was supplied for delivering the polymer solutions at a rate of 0.2 ml/h. The needle was also attached to an electrode of a high voltage power supplier (Institute of Beijing High Voltage Technology, China), which was responsible for applying a constant electrospinning voltage of 18 kV. The two random micro-and nano electrospun collagen membranes were collected with a grounded stainless metal drum wrapped with a piece of aluminum foil. The perpendicular distance between the syringe tip and the metal drum was fixed at 15 cm. Finally, the two micro-and nano electrospun collagen membranes, namely PDEC and CDEC, were obtained using the same parameters as above. A schematic diagram of the complete electrospinning process is shown in Fig.1.

Fig.1. here

2.3 Characterization of the PDEC

2.3.1 The morphology of PDEC and CDEC

A scanning electron microscopy (SEM, Hitachi S3000N, Hitachi, Ltd., Japan) was applied to observe the morphology of PDEC and CDEC qualitatively [28,30-31]. All

the specimens were coated with aurum and imaged at an accelerating voltage of 5 kV. Meanwhile, the AFM analysis was also used to characterize the morphology of PDEC, CDEC, collagen and gelatin specimens. It was conducted in air at room temperature on a Dimension 3100 Nanoscope IV equipped with silicon TESP cantilevers (Shimadzu SPM-9600, Japan) in noncontact (taping) mode [30]. 5 μL of the solutions with a concentration of 20 μg/ml (w/v) were dropped onto a fresh mica substrate and dried overnight in a desiccator at room temperature. For each sample, the analysis was made at five different points to confirm the consistency of the observed morphologies.

2.3.2 Electrophoretic Analysis

Electrophoretic patterns of the specimens were obtained via SDS–PAGE (Bio-Rad Powerpac 300) according to our previous report [31] with a slight modification. 7.5% resolving gel and 4% stacking gel were prepared for walking gel of the solutions at a concentration of 5 mg/mL. Finally the gel was stained for about 30 min with 0.25% Cooomassie brilliant blue R250 solution and destained with a 7.5% acetic acid/5% methanol solution until the bands were clear. Further, the purity of PDEC was also determined by BandScan Software 5.0.

2.3.3 FTIR spectra measurements

FTIR spectra was obtained from tablets containing 2 mg of PDEC, CDEC, collagen and gelatin specimens in approximately 100 mg of potassium bromide (KBr) with an FTIR spectrophotometer (Spectrum One, PerkinElmer, Inc., Waltham, MA) for secondary structural analysis. All spectra were collected by transmission mode at 2 cm^{-1} interval and in the wavelength range of 4000–400 cm^{-1} wavenumbers in a dry

atmosphere at room temperature [31].

2.3.4 Circular Dichroism (CD) Measurements

The PDEC, CDEC, collagen and gelatin solutions dissolved in 0.1M acetic acid with a concentration of 0.5 mg/mL were equilibrated at 25℃ before detection and scanned in a wavelength range from 185 to 250 nm. The molar ellipticity was recorded with a CD apparatus (Model 400, AVIV) [32].

2.3.5 Measurement of the Specific Intrinsic Viscosity

The specific intrinsic viscosities of the specimens mentioned above were measured with an Ubbelohde capillary viscometer at a constant-temperature bath (25.0± 0.1℃) according to our previous literature [30]. The specimens with a concentration of 0.5 mg/mL were first dissolved in 20mL 0.5M acetic acid solution, after that, 10 mL of the solutions mentioned above were diluted to yield four lower concentrations (0.4mg/ml, 0.25mg/ml, 0.225mg/ml, and 0.2mg/ml, respectively) made by the addition of an appropriate amount of 0.5M acetic acid to the stock solutions. The relative viscosities of all the specimens were calculated by the division of the flow times of the solutions by that of the pure solvent. All the measurements were performed in the range $1.1<\eta_r<2.5$ to provide typical data points (η_r means the solution-solvent viscosity ratio).

2.3.6 US–DSC Measurements

The specimens were measured on a VP-DSC microcalorimeter from Microcal Inc. with acetic acid interpreted as the reference. The solutions, with a concentration of 0.5 mg/mL, were degassed for 30 min at ambient temperature (25± 1℃) before the tests.

All the scans were carried out at a constant heating rate of 1℃ /min at temperatures ranging from 25 to 60℃ [33].

2.3.7 Crystallization characteristics

The crystallization characteristics of the specimens were tested by X-ray diffraction (XRD) analysis. XRD was conducted using a X′Pert Pro X-ray diffractometer (Netherlands). The parameters of the apparatus were set to the voltage 40 kV, the current 45mA. All the specimens were scanned in the range from 5° to 50°. [31, 34]

2.3.8 Tensile tests

Before the mechanical characteristics of PDEC and CDEC membranes were appraised with an electronic universal material tensile machine (UTM 6203, China) in ambient temperature at 20□ and humidity of 65%, the thickness of PDEC and CDEC was tested primordially using a manual micrometer with a resolution of 0.01 mm. Then each membrane was uniaxially stretched in the vertical direction at a constant speed of 10 mm/min and finally the values of tensile strength and elongation at break were obtained.

2.2.9 Cytotoxicity analysis of PDEC

The mitochondria activity of the fibroblasts seeded in the protein-coated plastic tissue culture plates was evaluated by MTT assay using a mouse-derived established cell line of L929 fibroblasts, which were purchased from West China Hospital, Sichuan University (China). Briefly, the two sterilized electrospun collagen, natural porcine collagen and gelatin were dissolved in PBS at a stock concentration of 10

μg/ml and then coated in the surface of each plastic tissue culture plate (24-well). Subsequently, the cells were inoculated into 24-well plates at the density of 1×10^4 cells/well in Dulbecco's modified Eagle medium (DMEM) supplemented with 1% (v/v) antibiotic solution and performed at 37 °C in humidified 95% air/5% CO_2 for 1, 3 and 5 days. Finally, using the (4, 5-dimethylthiazol-2yl)-2, 5-diphenyltetrazoliumbromide (MTT) assay, the viable cells cultured in each well were determined at the above days after cell seeding. Details of the methodology used in the MTT assay were previously reported. [31,35]

3. Results and discussion

3.1 The morphology of PDEC

Fig.2 and Fig.3 exhibit the morphological diversities of PDEC, CDEC, collagen and gelatin. SEM examination confirms the nanofibrous nature of the electrospun original membrane which shows that the diameter of PDEC membrane distributes in 0.06-2.40 μm, while Fig.2 (B) depicts that the fiber diameter of the CDEC presents more tiny than that of PDEC, which may imply that the mechanical property of PDEC is more superior that that of CDEC. All in all, the dimensions of the two electrospun collagen in the membrane range from nanometer to micrometer size. Fig.3 shows the morphological differences among the specimens observed by AFM. Typical topographies in the collagen fibrils are observed (Fig.3 A, B, D). Further, both the PDEC and collagen exhibit a three-dimensional netlike structure, where many curved molecules or microfibrils lie and are overlapped with one another [33], which may indicate that the electrospinning process of pADM does not destroy the basic fibrous

structure of native collagen. However, it is worthy to note that the PDEC molecules or fibrils seem to be more crowded obviously than that of the CDEC and exhibit meshy fibrous network topographies in Fig.3 (A). Furthermore, the average diameter of PDEC is far smaller than that of collagen. Above all, a very small amount of structural fragments that are simillar to the frame of gelatin (Fig.3 C) are found in Fig.3 (B), which indicates that the conformation of the PDEC may be disrupted to some extent and somehow the gelatin molecules are generated in the electro-spinning process. However, most of the fibrous structure of PDEC still remains compact and clear, which has already reached our requirments. Meanwhile, the porphyritic texture of CDEC is observed (Fig.3 E), which is just the same as gelatin and totally different from the PDEC.

Fig.2. and Fig.3. here

3.2 Electrophoretic Analysis

Fig.4 shows the SDS–PAGE patterns of collagen, PDEC and gelatin. It is obvious that the electrophoretic straps of two typical α-chains (α_1 and α_2) and the dimer of α-chains (β-chain) with a molecular weight of approximate 100 kDa and 200 kDa, respectively, are clearly visible in the SDS–PAGE patterns of collagen and PDEC specimens. However, compared to collagen, patterns with smaller molecular weights than 100 kDa in the PDEC are also found, which indicates that the PDEC specimen may be partially destroyed into gelatin, in other words, the conformation of PDEC tranforms from the triple helix to the random coil. Futher, BandScan Software 5.0 was also used to determine the purity of PDEC, and 15.89% of collagen was degraded into

gelatin. Moreover, the electrophoretic bands of gelatin are basically not very clear, which is just simillar to the bands of CDEC reported in the literature [14]. This phenomenon is consistent with that of AFM analysis to a certain degree. Based on the aforementioned results, it may be concluded that a certain amount of interhydrogen or intrahydrogen bonds within PDEC specimen, which plays a major role in maintaining the conformation of collagen molecules, may be broken and thus the structural integrity of PDEC is partly damaged, while collagen in the CDEC is almost degraded into gelatin. This is further in agreement with the results of the thermal stability and specific intrinsic viscosity.

Fig.4. here

3.3 FTIR spectra analysis

The secondary structure of the PDEC, CDEC, collagen and gelatin were investigated by Fourier transform infrared (FTIR) spectra considering that the FTIR spectra of protein molecules could be correlated directly to their backbone conformation [33]. As reported previously [36], the amide A and B bands of pure collagen center at 3400cm $^{-1}$ and 3082cm $^{-1}$, respectively [28, 31], which are mainly associated with the stretching vibrations of N-H groups. As shown in Fig.5, the amide I band at 1650 cm^{-1} arises predominantly from protein amide C=O stretching vibrations, while the amide II band at 1550 cm^{-1} is dominantly made up of amide N–H bending vibrations and C–N stretching vibrations (60% and 40% contribution to the peak, respectively). In addition, the amide III band at 1240 cm^{-1} is mainly attributed to the C-N stretching, N-H bending vibrations and wagging vibrations of CH_2 groups in the

glycine backbone and proline side chains [37]. It is obviously noted that the positions of main amide bands are still maintained as shown in Fig.5, especially the amide I band correlated to the helix structure of collagen [36]. The results above declare that the backbone of the PDEC does not change almostly, while both the reduction in the intensity of amide A, I, II and III peaks and narrowing of amide I band in the FTIR spectra of gelatin and CDEC are observed, which may represent the denaturation of collagen[38-42]. Furthermore, compared to collagen, the amide A bond of PDEC in Fig.5 appears to be more sharp which may have arisen from the partial disruption of hydrogen bonds within collagen molecules, resulting from the interactions between collagen and HIFP molecules.

It is also worthy to note that the absorbance bands at 1200-1450 cm^{-1} are closely related to the triple helical structure of collagen and it can be further used to quantify the denaturation of a collagen sample [43]. The absorption ratio of Amide III to 1450 cm^{-1}, denoted as A_{III}/A_{1450}, is also considered as a measurement of the preservation of structure integrity of collagen. Fig.5 shows that the PDEC has just a little lower value of A_{III}/A_{1454} than that of collagen, which is conceivable that the triple-helical conformation of PDEC is mostly retained. However, it is undeniable that a fractional structure of PDEC is destroyed into gelatin, and the results closely coincide with the AFM and electrophoretic analysis.

Fig.5. here

3.4 CD analysis

To further determine whether the structure integrity of PDEC was destroyed or

not, circular dichroism (CD) was performed to measure the structure of the specimens, as shown in Fig.6. It is well known that the denaturation of collagen or its helix destruction usually results in the disappearance of the positive band around 221 nm which is the characteristic of the collagen triple helix. Simultaneously, a negative trough around 198 nm also exists in the spectrum of collagen. The intensity ratio of the positive peak to the negative peak (Rpn) is commonly used to determine the conformation of collagen. Peak-to-peak variation of intensity ratio can reflect the changes in the structure of collagen to some extent. In general, when the collagen triple helix structure is completely destroyed, the positive summit will completely disappear, and the spectrum at ~198nm will also shift into lower wavelength. Further, a partially denatured collagen exhibits a spectrum with lower intensity of the peak at ~221 nm, as well as a lower value of Rpn. Fig.6 shows that both the intensity of the peak at ~221 nm and the Rpn value of PDEC decrease slightly compared with collagen, indicating that its triple helix structure is weakened mildly and somehow a little amount of gelatin may be generated. Furthermore, the Rpn value of PDEC remains reversely high, which illustrates that the triple helix structure of PDEC is still maintained. It may be because that fluoroalcohols can denature the structure of native collagen, which is strongly testified that electro-spinning of collagen out of fluoroalcohols results in the creation of gelatin. However, the multi-level aggregation structure of pADM hinders the destruction of collagen's structure by hexafluoroisopropanol molecules, which causes the slightly damage of the natural collagen's structure. Furthermore, the results of Young simulation of circular

dichroism are also analyzed and shown in Table 1. The structure of collagen contains 74.2%, 10.5% and 7.0% of α-helix, β-sheet structure and random coil structure, respectively, which is consistent with the literature reported [44]. Compared to collagen, a slightly higher content of β-sheet structure but less amount of α-helix stucture are presented in gelatin and CDEC. Meanwhile, their random coil structure is much more clear. However, a higher content of α-helix structure exists in PDEC and its β-turn structure is relatively less, which coincides with the early analysis. It may be because the β-turn structure in protein can be transformed into α-helix structure by hexafluoroisopropanol [45]. The effects of hexafluoroisopropanol on proteins are considered to be arised from its low polarity. The aggregation or clustering of hexafluoroisopropanol molecules provides a local nonpolar environment, where hydrophobic interactions are weakened but hydrogen bonds are strengthened. Further, this low polarity may weaken the intramolecular hydrophobic interactions that stabilize the inherent structure of proteins [14], but simultaneously strengthen electrostatic interactions such as hydrogen bonds, thus stabilizing secondary structure, particularly the α-helix structure, which is consistent with the results confirmed above.

Fig.6. here

Table 1 herre

3.5 The specific intrinsic viscosity of PDEC

Based on the measurement of the reduced viscosities of the collagen solutions in a concentration range of 0.20–0.50 mg/mL at 25℃, the specific intrinsic viscosities of

collagen, PDEC, CDEC and gelatin are shown in Fig.7. It is obvious that the specific intrinsic viscosity of PDEC (1.43 mL/mg) is slightly lower than that of collagen (1.20 mL/mg), but much higher than that of CDEC and gelatin, only 0.67 and 0.87 ml/mg, respectively. Apparently, this result correlates well with the value (1.40 mL/mg) reported in our previous work [28], and further demonstrate that the structure integrity of PDEC is still maintained to a large extent during the electrospinning process, which is considered as the foundation of the biological activity of collagen. Obviously, the results are consistent with that of electrophoresis analysis.

Fig.7. here

3.6 The thermal stability of PDEC

It was reported that US-DSC could be used to differentiate between collagen and gelatin, since microcalorimetry could sensitively detect the conformational changes of collagen in heating process. The thermal stability of the specimens was assessed by US-DSC analysis. As shown in Fig.8, there are two distinct peaks of collagen and PDEC, while just one broad peak exists in the stripe of CDEC. Nevertheless, gelatin exhibits only a smooth linear stripe. Generally, the heating transformation of collagen is considered to be the collapse of the collagen triple-helical structure into random coils, and the main endothermic peak is normally assigned to T*d*. Furthermore, there is usually a slight endothermic peak in the range from about 25 to 35℃ that is easy to be neglected and this peak is always interpreted as the pretransition temperature (T*p*). At the pretransition temperature, the triple-helical structure within collagen sample tends to be looser and more relax but still maintains its special triple-helical

configuration, which seems to be just ready for the denaturation process. The results show that the T*d* value of collagen and PDEC are 40.1 and 37.9℃, respectively. What's more, the strip of PDEC is totally different from CDEC and gelatin. In addition, T*p* of PDEC is also slightly lower, about 3℃ lower, than that of collagen. It is speculated that the aggregation of HIFP molecules could break the hydrogen bonds between the adjacent polypeptide chains of the collagen molecules, as demonstrated from CD analysis. However, T*d* of PDEC is still kept around 38℃, and this may suggest that the triple helix structure of PDEC is almost remained and is considered to be acceptable for biomedical use.

Fig.8. here

3.7 The crystallinity of PDEC

The crystallinity of collagen, PDEC, CDEC and gelatin was assessed by XRD analysis, as shown in Fig.9. According to the literature [31], it is reported that collagen has three different diffraction peaks. The relatively sharp diffraction peak (labeled C peak) is yielded between 5° and 10°, indicating an intermolecular lateral packing distance among the peptide chains of collagen molecules. The second broad peak at around 20° (A_1 peak) results from the diffuse scattering, and a very small diffraction peak at 30° to 35° (A_2 peak) represents the distance among the adjacent amino acid residues of the triple helix spiralled along the central axis. Therefore, we believe that the two-phase structure exists in the structure of collagen, namely one is more structured phase, corresponding to C peak, and another phase constitution is amorphous, corresponding to A_l peak, which accounts for the "Core-shell" theory.

Generally, Bragg equation ($2d\sin\theta=\lambda$) can be used to describe the X-ray diffraction pattern of different materials, thus it appears that *d* values corresponding to the diffraction peak can be calculated if the X-ray wavelength (Cu target is used, λ=0.154nm) and the angle θ are obtained. As shown in Table 2, intermolecular lateral packing distance among the PDEC molecular chains is 1.203 nm, which is slightly larger than that of swine type I collagen but much smaller than that of CDEC (1.351 nm). This may indicate that the hydrogen bonds and van der Waals forces among the peptide chains of PDEC molecules are weakened and thus the gaps among the PDEC molecular chains increase. Simultaneously, the peak C of PDEC appears to be more broadened than that of collagen specimen. This broadening can be attributed to an promotion in the disorder, a reduction in the crystallite size, or a combination of the two [33]. In an ideal α-helix, each turn of the coil contains 3.6 amino acid residues (n = 0.36), and the screw pitch is 0.54 nm (p = 5.4Å); along the central axis of the spiral, the distance among adjacent amino acid residues is 0.15 nm (1.5 Å). As is known, the helical structure of collagen is different from the general α-helix structure. Generally, in the helical structure of collagen, each loop-helix contains 3.3 amino acid residues (n = 3.3), and the screw pitch is 0.96nm (p = 9.6Å). Moreover, along the central axis of the coil, the distance of adjacent amino acid residues is 0.29nm (2.9Å). Table 2 shows that the distance of adjacent amino acid residues in the helical structure of PDEC is 0.284nm, which fully confirms that the PDEC still better maintains its helical structure.

Fig.9. here

Table 2 here

3.8 Mechanical properties

The mechanical properties are significant for the tissue engineering scaffolds. Generally, the inherent structure and composition of biomaterials is closely relevant to their mechanical properties. The relative mechanical parameters, average diameter and the thickness of the PDEC and CDEC are presented in Table 3. It could be seen that both the tensile strength and elongation at break of the PDEC are visibly higher than those of the CDEC. Moreover, the average diameter of PDEC measured experimentally by using SEM also seems to be more large. We infer that the results occur due to the following aspects: First, the fibers of PDEC intertwine with each other more closely and its three dimensional netlike structure seems more tight than that of CDEC, which is extremely conducive to improving the mechanical properties. Second, the more burly fibers also contribute to the superior mechanical properties of PDEC. Third, as testified in the previous analysis, the triple helix structure of PDEC is almost remained, which also has significant effects on its mechanical properties.

Table 3 here

3.9 Cytocompatibility analysis

The biocompatibility is crucial for an ideal tissue engineering scaffold in its application and the biological activity of collagen is based on its structural integrity. The preliminary cytotoxicity of the PDEC, CDEC, gelatin and natural porcine

collagen in this study was evaluated with the method of colorimetric assay. Fig.10 illustrates the effect of various coated specimens on the proliferation of L929 fibroblasts. After fibroblasts are cultivated in the coated plates for one day, the optical density of the PDEC and collagen performs no statistically significant change but slightly higher than that of CDEC and gelatin, whereas quantitative assessment of the cytotoxicity shows relatively higher optical density than that of CDEC, gelatin and control groups after cultured for 3 and 5 days. During the culture of L929 fibroblasts, fibroblasts were totally engaged in adhering onto the bottom of the tissue culture plates, and the proliferation of fibroblasts had not yet started in the 1st day. Furthermore, it is still worthy to note that the optical density of the PDEC is slightly lower than that of natural porcine collagen in the third and fifth day, even though the biological properties of the PDEC and porcine collagen are superior to the CDEC and gelatin obviously. As demonstrated previously in this study, the main conformation of the PDEC is still remained, although a small amount of the PDEC is destroyed into gelatin. Hence, we would like to draw the conclusion that the PDEC still maintains its special biological activity due to its reserved integrated triple helix structure, which may be suitable to be a tissue engineering scaffold.

Fig.10. here

Conclusion

In this study, we demonstrated that the pADM-derived electrospun collagen could almost maintain its integral triple helix structure. However, a small amount of PDEC destroyed into gelatin was demonstrated by SDS-PAGE, the specific intrinsic

viscosity, CD and AFM analysis. There are little differences on thermal stability and crystallization between the PDEC and collagen. Therefore, the structure of PDEC we conducted is totally different from CDEC and the mechanical properties of PDEC are significantly enhanced compared to that of CDEC. Further, the biocompatibility of the PDEC is estimated with fibroblast proliferation and the results suggest that the PDEC can promote the proliferation and growth of fibroblasts, which may also indicate that the triple-helical conformation of PDEC is mostly retained. Taken as a whole, these results may pave the way for developing a novel electrospun collagen scaffold for tissue engineering scaffolds.

Acknowledgement

The financial support of National Natural Science Foundation of China (contract grant number 51473001) and Ph.D. Programs Foundation of Ministry of Education of China (contract grant number 20130181110092) are gratefully acknowledged.

References

1 A. Frenot, and I. S. Chronakis, *Current Opinion in Colloid and Interface Science*, 2003, **677**, 64 –75.

2 Z. M. Huang, Y. Z. Zhang, M. Kotaki, and S. Ramakrishna. *Composites Science and Technology*, 2003, **63**, 2223–2253.

3 D. Li, and Y. Xia. *Advanced Materials*, 2004, **16**, 1151–1170.

4 S. Ramakrishna, K. Fujihara, W. E. Teo, T. Yong, Z. Ma, and R.E. Ramakrishna.

Materials Today, 2006, **9**, 40 –50.

5 H. J. Jin, S. V. Fridrikh, G. C. Rutledge, and D. I. Kaplan, *Biomacromolecules*, 2002, **3**, 1233–1239.

6 M. S. Khil, D. I. Cha, H. Y. Kim, I. S. Kim, and N. Bhattarai, J*ournal of Biomedical Materials Research Part (B)*, 2003, **67**, 675–679.

7 J. Zeng, X. Xu, X. Chen, Q. Liang, X. Bian, L. Yang, et al., *Journal of Controlled Release*, 2003, **92**, 227–231.

8 Z. G. Chen, X. M. Mo, and C. L. He, *Carbohydrate Polymers*, 2008, **72**, 410–418

9 Q. P. Pham, U. Sharma, and A. G. Mikos, *Tissue Engineering*, 2006, **12**, 693 1197–1211

10 L. Huang, K. Nagapudi, R. P. Apkarian and E. L. Chaikof, *Journal of Biomaterials Science-polymer Edition*, 2001, **12**, 979–993.

11 J. A. Matthews, G. E. Wnek, D. G. Simpson and G. L. Bowlin, *Biomacromolecules*, 2002, **3**, 232–238.

12 B. Dong, O. Arnoult, M. E. Smith and G. E. Wnek, *Macromolecular Rapid Communications*, 2009, **30**, 539–542

13 L.M. Meng, A. Oliver, S. Meghan, and E.W. Gary, *Journal of Materials Chemistry*, 2012, **22**, 19412–19417

14 I. Z. Dimitrios, T. K. Shih, S. Y. Y. Elijah, K. E. Andrew, W. T. Yen, Y .L. Y. Lin, et al., *Biomaterials*, 2008, **29**, 2293-2305

15 A.J. Bailey, *Journal of the Society of Leather Technologists and Chemists*, 1992, **76**, 111-127.

16 A. Finch, P. J. Gardner, D. A. Ledward, and S. Menashi, *Biochimicaet Biophysica Acta (BBA)-Protein Structure*, 1974, **365**, 400-404.

17 W. Friess, and G. Lee, *Biomaterials*, 1996, **17**, 2289-2294.

18 L. Buttafoco, N.G. Kolkman, P. Engbers-Buijtenhuijs, A.A. Poot, P. J. Dijkstra, I. Vermes, et al., *Biomaterials*, 2006, **27**, 724-734.

19 S. P. Zhong, W. E. Teo, X. Zhu, R. Beuerman, S. Ramakrishna, and L.Y. L. Yung, *Materials Science and Engineering C*, 2007, **27**, 262-266.

20 S. Kidoaki, IK. IK. Kwon, and T. Matsuda, *Biomaterials*, 2005, **26**, 37-46

21 A. Veis, J. Anesey and J. Cohen, *Archives of Biochemistry and Biophysics*, 1961, **94**, 20-31.

22 M.C. Bottino, V. Thomas, M.V. Jose, D.R. Dean, and G.M. Janowski, *Journal of Biomedical Materials Research B*, 2010, **95**, 276–282.

23 X. Zhang, J. Yang, Y. Li, S. Liu, K. Long, Q. Zhao, Y. Zhang, Z. Deng, and Y. Jin, *Tissue Engineering Part C Methods*, 2011, **17**, 423–433.

24 H. Zhao, G. Wang, S. Hu, J. Cui, N. Ren, D. Liu, et al., *Tissue Engineering Part A*, 2011, **17**, 765–776.

25 E.L. Heck, P.R. Bergstresser and C.R. Baxter, *Trauma*, 1985, **25**, 106-112.

26 D.J. Wainwright, M. Madden, A. Luterman, et al., *Journal of Burn Care & Rehabilitation*, 1996, **17**, 124-136.

27 J.M. Gryskiewicz, R.J. Rohrich, and B.J. Reagen, *Plastic and Reconstructive Surgery*, 2001, **107**, 561-570.

28 Y. Hu, L. Liu, W. Dan, N. Dan, Z. Gu and X. Yu, *International Journal of*

Biological Macromolecules, 2013, **55**, 221–230

29 H. Lin, W. Dan and Dan N., *Journal of Applied Polymer Science*, 2012, **23**, 2753

30 Y. Chen, L. D. Yan, T. Yuan, Q. Y. Zhang and H.J. Fan, *Journal of Applied Polymer Science*, 2011, **119**, 1532–1541

31 Y. H, L. Liu, W. Dan, N. Dan, and Z. Gu, *Journal of Applied Polymer Science*, 2013, **130**, 2245–2256

32 Y. Hu, L. Liu, Z. Gu, W. Dan, N. Dan and X. Yu, *Carbohydrate Polymers*, 2014, **102**, 324–332

33 A. Lungu, M.G. Albu, I.C. Stancu, N.M. Florea, E. Vasile, and H. Iovu, *Journal of Applied Polymer Science*, 2013, **127**, 2269–2279.

34 W. Song, D.C. Markel, S. Wang, T. Shi, G. Mao and W. Ren, *Nanotechnology*, 2012, **23**, 115101.

35 Y. Xu, L. Li, X. Yu, Z. Gu, and X. Zhang, Carbohydrate Polymers, 2012, **87**, 1589–1595.

36 M.E. Andrews, J. Murali, C. Muralidharan, W. Madhulata and R. Jayakumar, *Colloid & Polymer Science*,2003, **281**, 766–770.

37 L. He, C. Mu, J. Shi, Q. Zhang, B. Shi and W. Lin, *International Journal of Biological Macromolecules*, 2011, **48**, 354–359.

38 W. Friess and G. Lee, *Biomaterials*, 1996, **17**, 2289–2294.

39 D. A. Prystupa and A. M. Donald, *Polymer Gels and Networks*, 1996, **4**, 87–110.

40 K. J. Payne and A. Veis, *Biopolymers*, 1988, **27**, 1749–1760.

41 A. George and A. Veis, *Biochemistry*, 1991, **30**, 2372–2377.

42 V. Renugopalakrishnan, G. Chandarakasan, S. Moore, T. B. Hutson, C.V. Berney and S.B. Ravejendra, *Macromolecules*, 1989, **22**, 4124–4124.

43 F. J. O'Brien, M. G. Haugh and M. J. Jaasma, *Journal of Biomedical Materials Research Part A*, 2009, **89A**, 363–369

44 B. Peng, *Journal of Imaging Science and Technology*, 1993, **37**, 380-385.

45 D.P. Hong, H. Masaru, K. Ryoichi and G. Yuji, *Journal of the American Chemical Society*, 1999, **121**, 8427-8433

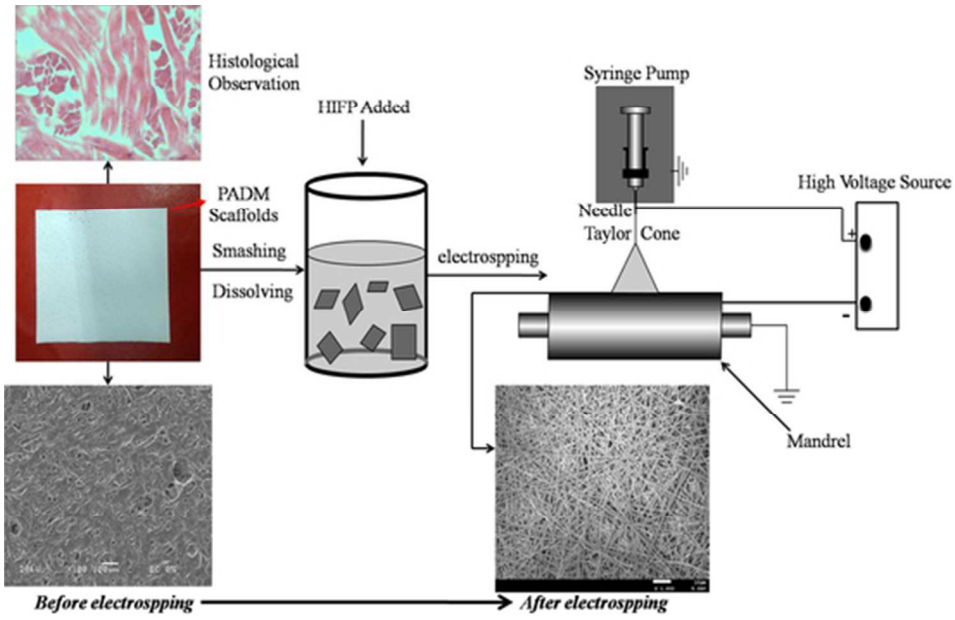

Fig.1. Schematic illustration showing the process of electrospinning described in this study
49x30mm (300 x 300 DPI)

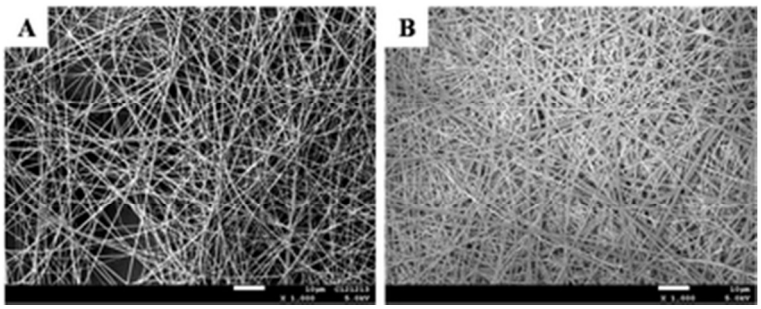

Fig.2. SEM images of CDEC (A) and PDEC (B)
31x12mm (300 x 300 DPI)

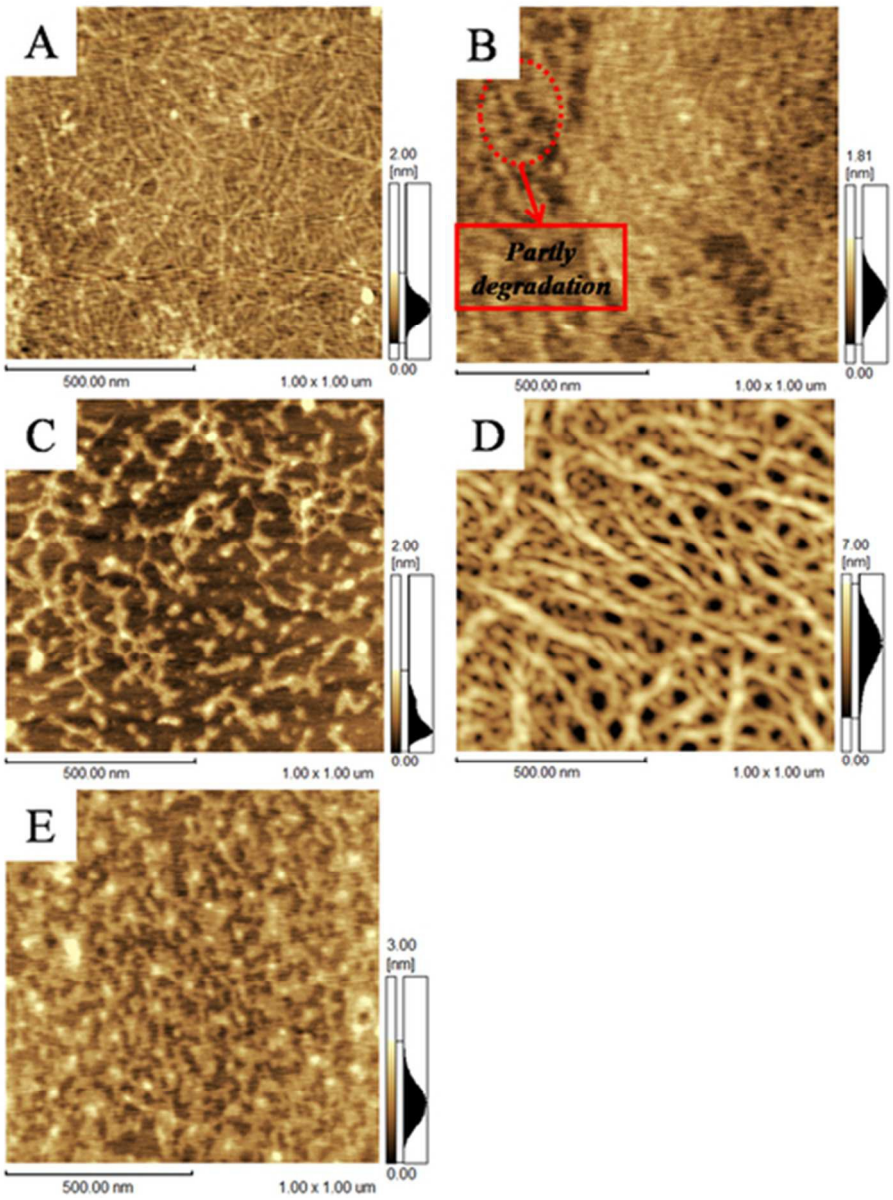

Fig.3. AFM images of PDEC (A,B), gelatin (C), collagen (D) and CDEC (E)
39x52mm (300 x 300 DPI)

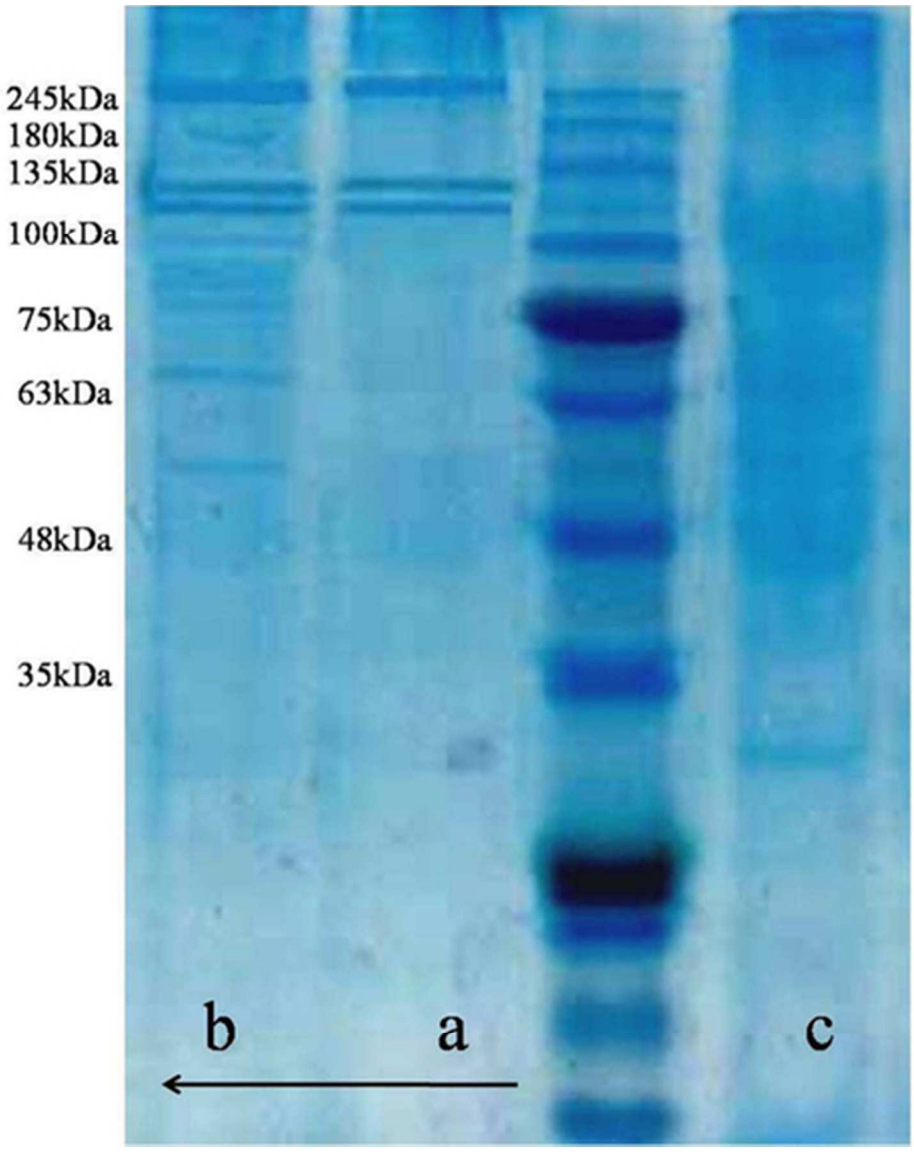

Fig.4. SDS–PAGE analysis of collagen (a), PDEC (b) and gelatin (c)
39x48mm (300 x 300 DPI)

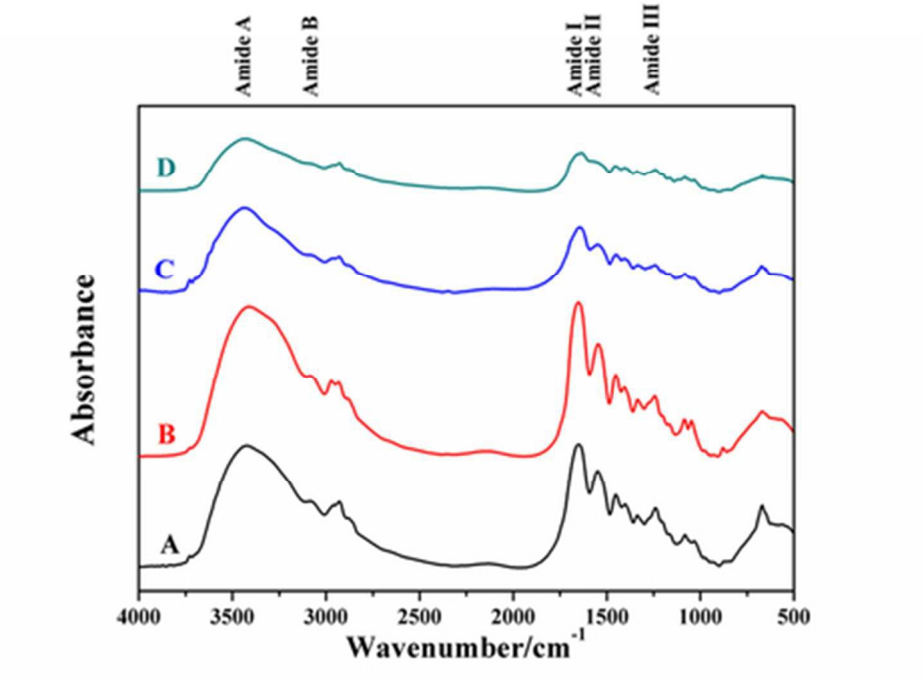

Fig.5 FTIR spectra of collagen (A), PDEC (B), gelatin (C) and CDEC (D)
38x30mm (300 x 300 DPI)

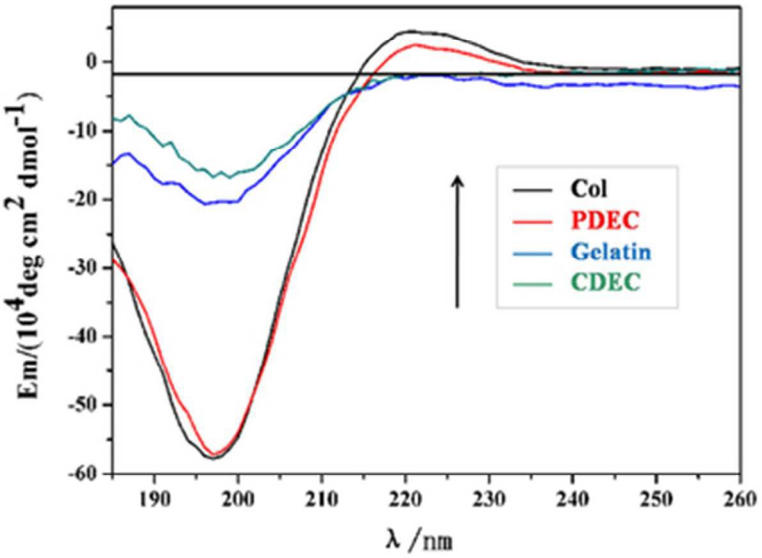

Fig.6. CD spectra of collagen, PDEC, gelatin and CDEC
38x27mm (300 x 300 DPI)

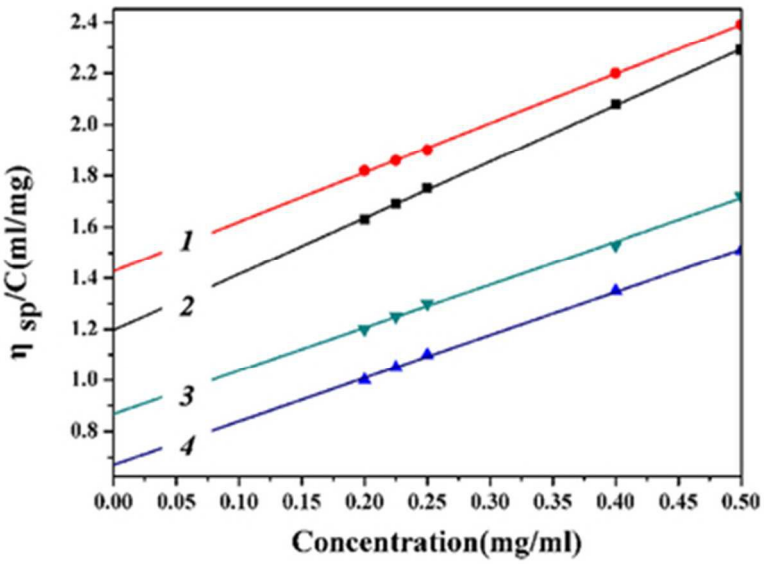

Fig.7. The specific intrinsic viscosity of collagen (1), PDEC (2), CDEC (3) and gelatin (4)
38x27mm (300 x 300 DPI)

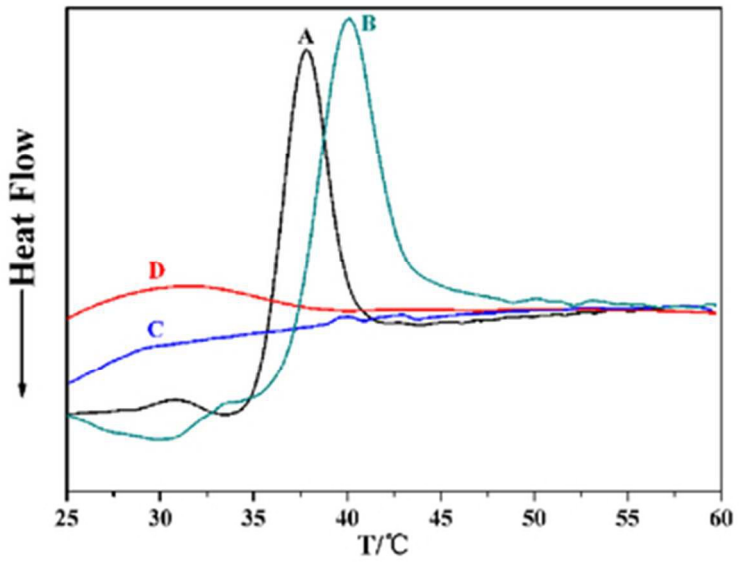

Fig.8. The thermal stability of PDEC (A), collagen (B), gelatin (C) and CDEC (D)
38x27mm (300 x 300 DPI)

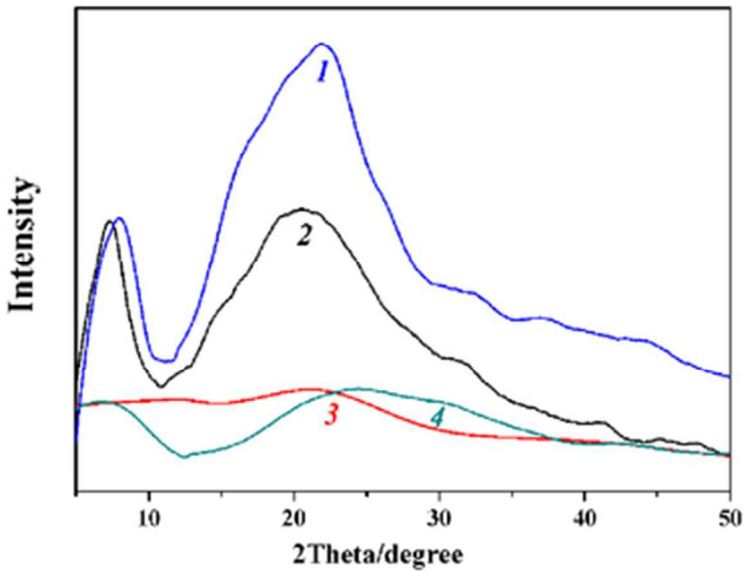

Fig.9. The crystallinity of collagen (1), PDEC (2), gelatin (3) and CDEC (4)
38x27mm (300 x 300 DPI)

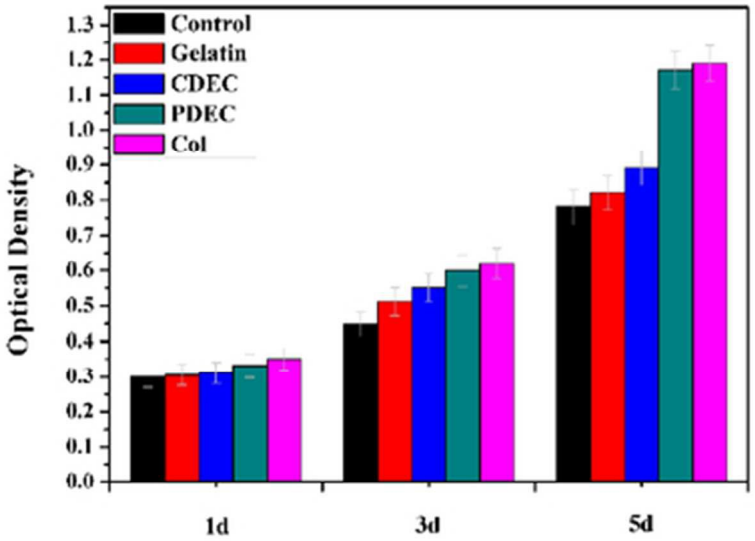

Fig.10. Proliferation of the fibroblasts on the protein-coated culture plates over a period of 5 days
39x27mm (300 x 300 DPI)

Table.1 The results of Young simulation of circular dichroism

Specimens	α-helix	β-sheet	β-turn	Radom coil	Total sum
PDEC	85.6%	1.8%	2.1%	10.5%	100%
Collagen	74.2%	1.2%	7.0%	17.6%	100%
CDEC	15.3%	50.5%	7.8%	26.4%	100%
gelatin	1.3%	62.0%	8.3%	28.4%	100%

Table 2 *d* values of diffraction peaks in X-ray diffraction diagram of collagen, PDEC and CDEC

Specimens	Parameters	Peak C	Peak A_1	Peak A_2
PDEC	Peak position (2θ°)	7.355	20.641	31.52
	d values (nm)	1.203	0.430	0.284
collagen	Peak position (2θ°)	8.096	22.004	32.144
	d values (nm)	1.092	0.403	0.278
CDEC	Peak position (2θ°)	6.54	26.21	—
	d values (nm)	1.351	0.340	—

Table 3 Parameters of mechanical property of PDEC and CDEC

	Thickness (μm)	***Tensile strength (MPa)***	***Elongation at break (%)***	***average diameter (μm)***
PDEC	30±5	26.36±5.7	148.3±12.31	1.17±1.23
CDEC	30±3	5.69±1.24	105.6±10.45	0.24±0.19